

Tensile and Compressive Microspecimen Testing of Bulk Nanoporous Gold

T. John Balk, Chris Eberl, Ye Sun, Kevin J. Hemker, and Daniel S. Gianola

Nanoporous gold (np-Au) is a macroscopically brittle material, which poses difficulties for tensile testing of bulk specimens. By combining a fabrication approach that minimizes cracking in bulk np-Au and a microspecimen test technique that permits small testing volumes, both tension and compression tests were performed on sub-millimeter gage thicknesses of np-Au. Compressive strength was higher than tensile strength, as would be expected for a brittle material, but all strength values were significantly lower than literature values for nanoindentation testing. Measured elastic modulus was nearly the same in tension and compression, and was much lower than Gibson-Ashby scaling relations would predict for porous gold with this density.

INTRODUCTION

The ease of fabrication and novel behavior exhibited by nanoporous gold (np-Au) have made this material an increasingly popular research subject. The nanoscale structure of pores and ligaments offers a high surface-to-volume ratio and, combined with the chemical properties of Au, suggest attractive properties for applications such as catalysis,¹ sensing,²⁻⁴ capacitance,⁵ and surface plasmon resonance.⁶ However, producing np-Au that is strong, tough and has good mechanical integrity has not yet been achieved. Although Au is a highly ductile metal, np-Au fails in a macroscopically brittle manner,⁷ which makes specimen handling difficult and poses severe constraints on mechanical testing. Previous reports of failure of np-Au investigated with three-point bend testing⁷ determined that samples significantly larger than their intrinsic pore size are more brittle. Thus, bulk samples of np-Au have a strong tenden-

cy to crack and undergo catastrophic failure when loaded in tension. Nonetheless, direct uniaxial tensile testing is the preferred method of assessing

material ductility, as damage evolution can give rise to signatures of apparent ductility during compression testing.

A second challenge associated with mechanical testing of bulk np-Au is the volume contraction and cracking that typically occur during dealloying. The dealloying process is used to leach a sacrificial element (in this case Ag) from a precursor alloy (Au₃₀Ag₇₀), which is followed by surface diffusion of Au and agglomeration of Au adatoms into clusters that eventually form the interconnected ligaments of the nanoporous structure.² The removal of 70% of the atoms from the original material is usually accompanied by a significant volume contraction, up to 30%.⁸ Often this contraction leads to intergranular cracking, which is exacerbated by the brittle behavior of np-Au. Recently, a two-step method for dealloying was developed.⁹ This approach avoids both volume contraction and cracking in bulk np-Au samples, and facilitates the processing of test specimens that can withstand tensile loading.

This paper presents tension and compression test results from microsamples of bulk np-Au that were processed to mitigate crack formation. These findings are discussed in relation to other studies of np-Au mechanical behavior. Most of the results in the scientific literature were obtained from nanoindentation of bulk np-Au, which delivers hardness values of ~150 MPa for as-dealloyed material with a ligament width of ~10–20 nm.^{10,11} Given the assumption of a near-zero Poisson's ratio for highly porous materials, the hardness value H measured during indentation is generally taken to be equal to the compressive yield strength σ_y , in contrast to the Tabor relation $\sigma_y = H/3$ commonly invoked for solid met-

How would you...

...describe the overall significance of this paper?

Nanoporous gold, an open-cell material with nanoscale pores and ligaments, is a promising material for sensing or catalysis. However, it is extremely fragile, exhibiting macroscopic brittleness. For the first time, nanoporous gold has been tested in tension to determine elastic modulus and yield/fracture strength. Elastic modulus was less than half the value predicted by classic scaling equations for porous materials, and the measured yield/fracture strengths in tension and compression were significantly lower than values reported in the literature and obtained from indentation tests.

...describe this work to a materials science and engineering professional with no experience in your technical specialty?

In this study, millimeter-scale specimens of nanoporous gold were tested in tension and compression, resulting in consistent strength and modulus values much lower than expected. Tensile testing showed that nanoporous gold has very little macroscopic ductility, even though individual ligaments undergo extensive plastic deformation.

...describe this work to a layperson?

Porous materials are typically weaker than fully dense materials. However, nanoporous gold, which has the structure of a kitchen sponge but with pores and ligaments only 10 nm in diameter, has been reported to have extremely high strength levels. In this study, nanoporous gold samples were tested mechanically and it was found that the material is actually not as stiff or strong as reported by other groups.

als. Another study of np-Au mechanical behavior utilized micropillars prepared with a focused ion beam, which exhibited a compressive yield strength of 100 MPa.¹² More recently, compression testing of millimeter-scale specimens revealed relatively low strength values (<30 MPa) in np-Au that exhibited large plastic strain.¹³ In the current study, the measured compressive and tensile yield strengths were both much lower than strength values derived from nanoindentation. A significant advantage of microspecimen testing is the ability to precisely measure elastic modulus in sub-millimeter gage sections, and the average moduli determined here were significantly lower than predicted by porous material scaling relations.¹⁴

MICROSPECIMENS OF BULK NANOPOROUS GOLD

Pellets ($\sim 5 \times 5 \times 5 \text{ mm}^3$) of a precursor alloy with composition $\text{Au}_{30}\text{Ag}_{70}$ were purchased from Kurt J. Lesker Co. The pellets were cold-rolled with a total reduction of 80%, corresponding to a true strain of 1.6, resulting in a sheet thickness of $\sim 1 \text{ mm}$. After this, they were annealed at 850°C for 100 h in order to relieve stress and achieve a coarse grain size, which ranged from 20 to 250 μm . The sheets were then ground and polished to a thickness ranging from 50 to 500 μm (most samples were 150 to 450 μm thick).

Microspecimens for both uniaxial tensile and compressive mechanical testing were fabricated by sinking electro-discharge machining of the bulk $\text{Au}_{30}\text{Ag}_{70}$ slices. This resulted in specimens with a gage width of $\sim 430 \mu\text{m}$, as measured by calibrated optical microscopy. The microspecimens were machined into a dogbone geometry as shown in Figure 1, typically used for tension testing,¹⁵ with large gripping sections at both ends and a straight gage section. Specimens for both tensile and compressive testing were nominally identical, although different gripping techniques were used (see below).

Dealloying of microspecimens was performed using the multistep method described in Reference 9. The extent of dealloying (i.e., amount of Ag removed in each step) varied for different samples. Therefore, each sample was dealloyed in a series of etchant solutions

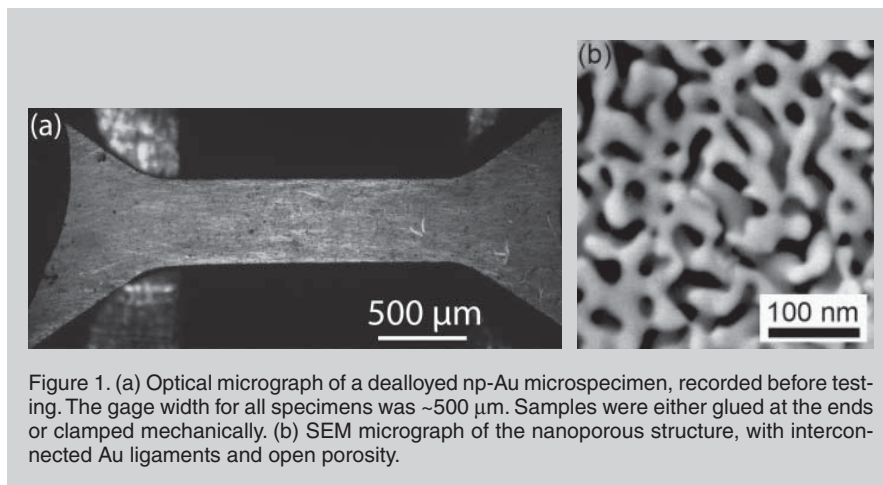


Figure 1. (a) Optical micrograph of a dealloyed np-Au microspecimen, recorded before testing. The gage width for all specimens was $\sim 500 \mu\text{m}$. Samples were either glued at the ends or clamped mechanically. (b) SEM micrograph of the nanoporous structure, with interconnected Au ligaments and open porosity.

with $\text{HNO}_3:\text{H}_2\text{O}$ ratios of 1:4, 1:3, 1:2 and finally concentrated HNO_3 . Some samples were dealloyed with fewer etchant solutions. Dealloying was performed until the dealloying current was negligible and the measured mass loss indicated that nearly all Ag had been removed. The remnant Ag content was typically less than 2 at.%, but did range up to 7 at.% for one sample. Figure 1 presents an optical micrograph of a representative microspecimen in the as-dealloyed state, which was crack-free and did not experience volume contraction. Average ligament width of the np-Au samples ranged from 20 to 35 nm, as determined by measurement of scanning electron microscopy (SEM) images such as that shown in Figure 1b. Based on the measured ligament width and relative density (30%) of the bulk np-Au sample, an average pore size of 17 to 29 nm was calculated. Thus, at least 1,000 cells (pore/ligament pairs) and 1–10 grains spanned the thickness of each microspecimen.

MICROSPECIMEN TEST PROCEDURE

A custom-built mechanical testing apparatus¹⁶ was employed to assess the response of the dealloyed np-Au microspecimens. The major components of this system include a single-axis piezoelectrically actuated screw-driven motor for displacement actuation, a five-axis motor for alignment of the microspecimen, a miniature load cell for force measurement, an air bearing for minimizing friction during loading, and a high-resolution optical microscope equipped with a digital camera for strain measurement. The gage section of each specimen was aligned with the

loading axis of the test system, using the five-axis stage and optical microscope. High-viscosity, ultraviolet-curable glue was used to affix the specimens to the grips. The high viscosity prevented seepage of the glue through the porous material. The np-Au microspecimen in Figure 1 is shown on the test stage. To ensure reliable gripping and avoid crushing in the grips, the tension and compression specimens were either glued or clamped to the stage. Gage lengths were shorter for compression specimens to avoid buckling during testing. All experiments were conducted at a nominal strain rate of 10^{-5} s^{-1} .

Digital images were captured with a 6-megapixel camera during mechanical testing, and strain in the microspecimens was calculated from these images using digital image correlation (DIC). Digital image correlation enables non-contact strain measurement by calculating displacement shifts between reference and deformed images, with sub-pixel resolution. This method has been utilized by many researchers and the theory described in detail elsewhere.^{17–19} Digital image correlation has the advantage of full-field capability with local fidelity (e.g., ability to detect strain heterogeneities near grain boundaries and stress concentrations). The full-field information computed from images obtained during mechanical testing provided information on the strain evolution in both in-plane directions of the images, and allowed for the direct quantification of Young's modulus and Poisson's ratio. A DIC software suite developed by the authors and implemented using MATLAB²⁰ was utilized in this study. The np-Au mi-

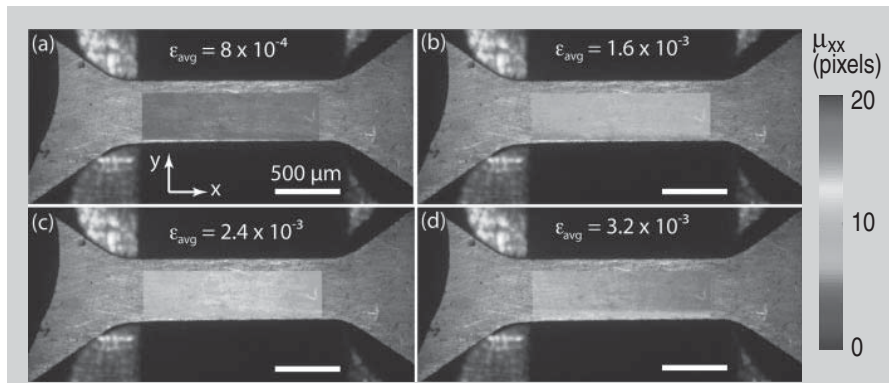


Figure 2. Displacement fields calculated using DIC and superimposed on optical micrographs of microspecimen S1 during tension testing. The average strain value is indicated in each image. Displacement gradients, and therefore strain, are quite uniform along the gage length. Poisson's ratio can be calculated from the biaxial strain fields. Please see on-line content at www.tms.org/pubs/journals/JOM/0912/balk-0912.html for a color movie that shows the evolving displacement field during the tension test.



crossspecimens provided sufficient natural surface contrast for high-resolution DIC, and thus the application of surface markers at the micrometer length scale was not necessary. A representative snapshot of full displacement fields and calculated strain at various stages of an np-Au microspecimen tensile test is shown in Figure 2. The gradient of the displacement field is related to axial strain, which is relatively uniform throughout the gage section, especially at low strain (Figure 2a). The displacement gradient is oriented along the tensile axis of the microspecimen, even at higher average strains (Figures 2c–d), indicating good sample alignment. The full-field characterization of displacement and strain provides access to the biaxial strain state, thereby allowing calculation of Poisson's ratio. It should be noted that the strain measurement employed here does not have the fidelity to resolve local heterogeneities at the length scale of individual ligaments. Nonetheless, tracking the displacement and strain fields (as shown in Figure 2) facilitates the accurate calculation of mechanical properties and also allows identification of testing abnormalities such as microspecimen buckling or slip within the grips. Artifacts due to these effects can thus be eliminated, yielding higher quality test data.

TENSILE BEHAVIOR

Microspecimen test techniques were employed for both tensile and compressive mechanical tests of bulk np-Au. Tensile test specimens exhibited little to no plasticity, due to the macroscopic-

cally brittle nature of np-Au deformation. Nonetheless, elastic properties and fracture strength were measured in multiple specimens. All tensile microspecimens demonstrated a linear elastic response, and only one specimen appeared to undergo limited plastic deformation. Figure 3 shows an engineering stress-strain curve for np-Au loaded in tension. A linear fit accurately described the test data, which for this specimen gave a Young's modulus of 3.2 GPa. As described previously, DIC allowed the calculation of the biaxial strain state during testing, which was utilized to compute Poisson's ratio ν of bulk np-Au under tension ($\nu = 0.15 \pm 0.02$ for this specimen, where the error bounds represent the cumulative uncertainties associated with strain measurement).

No appreciable tensile ductility was measured in most np-Au specimens, as seen for example in the stress-strain

curve of Figure 3. Tensile specimens typically fractured at the transition from the straight gage section to the gripping ears, which is where stress is locally concentrated. Thus, the tensile strengths measured here are probably a lower limit for the true fracture strength. Given the brittle nature of np-Au, the effects of subtle testing misalignments are generally exacerbated by stress concentrations from specimen geometry. Indeed, the tensile specimen that generated the data for Figure 3 was re-tested upon fracturing at the fillet (at a nominal strength of 11 MPa) by gripping the fractured end of the gage section with high-viscosity glue. When loaded again in tension, the microspecimen fractured in the middle of the gage section at a stress of 14 MPa, nearly 30% higher than the first test. During this second test, the specimen exhibited an apparent yield point (at 12 MPa) and a limited amount of plastic deformation before it fractured. This behavior may be attributed to the population of defects within the np-Au microspecimen (i.e., the weakest area failed first) and subsequent fracture required increasing amounts of stress as the defect population shrank. These mechanical test data are summarized in Table I, along with the data for other microspecimens tested in tension and compression.

Using three-point bend testing of millimeter-scale samples, Li and Sieradzki investigated the fracture behavior of bulk np-Au.⁷ They determined a fracture strength of 8.2 MPa for a ligament size of 18 nm. For np-Au with larger ligaments (60 nm), their

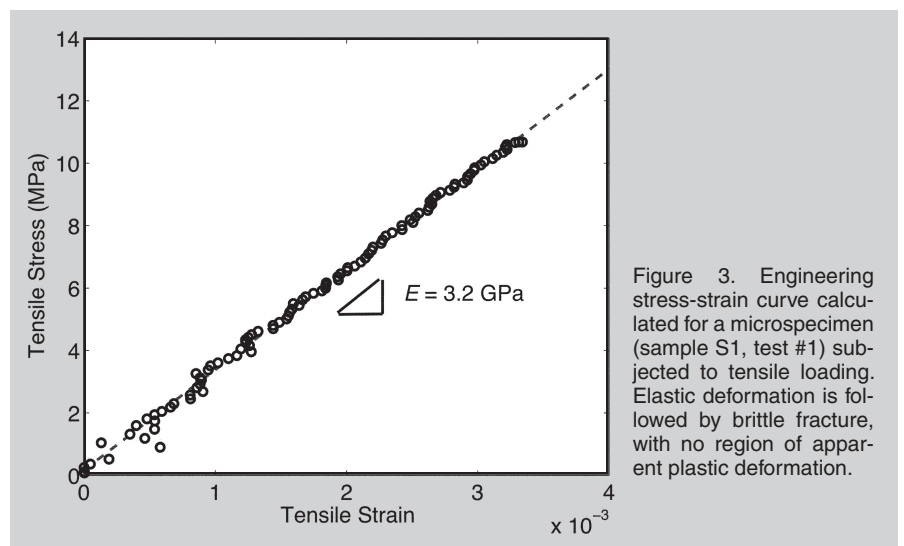


Figure 3. Engineering stress-strain curve calculated for a microspecimen (sample S1, test #1) subjected to tensile loading. Elastic deformation is followed by brittle fracture, with no region of apparent plastic deformation.

measure of fracture strength rose to 12 MPa. These values are quite close to the values of tensile yield and fracture strengths measured in the current study (see Table I), for which the np-Au ligament size ranged from 20 to 35 nm.

Figure 4 shows a sequence of initial crack formation and propagation from the specimen fillet during the microspecimen tensile test for Figure 3. No pre-existing cracks were seen before the test (Figure 4a). After elastic deformation had occurred, a small crack began to propagate along the maximum expected stress gradient at the fillet (Figure 4b), ultimately running perpendicular to the tensile axis. Approximately 10 s elapsed between Figures 4b and 4c, corresponding to a gage displacement of 0.25 μm . The crack advanced only slightly during this time. However, subsequent crack propagation was rapid, resulting in the complete fracture of the gage section as seen in Figure 4d. The interval between Figures 4c and 4d was ~ 5 s (0.125 μm gage displacement).

Although the macroscopic behavior of tensile microspecimens was brittle, the failure of individual ligaments was ductile, as would be expected for Au. A microspecimen tested to failure in tension is shown in Figure 5. The fracture surface in Figure 5a corresponds to brittle failure. However, observation of the ligament structure at the crack surface reveals that individual ligaments

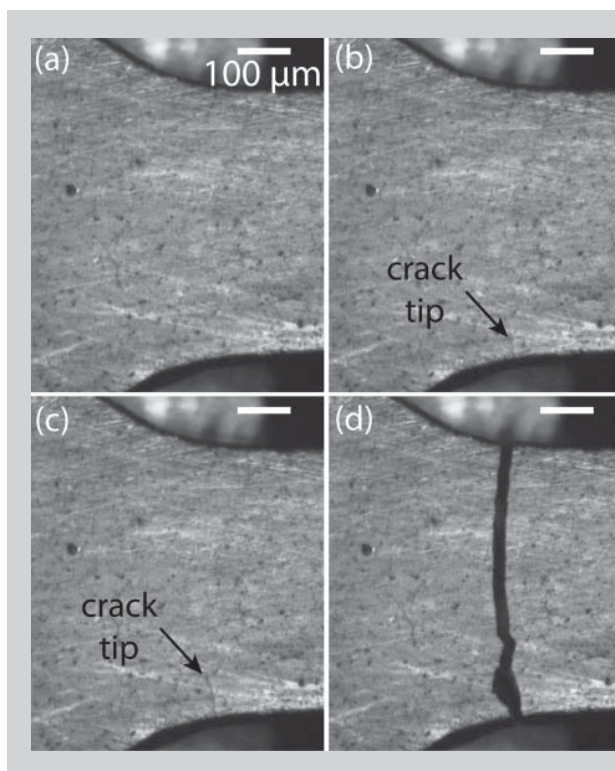


Figure 4. Optical micrographs obtained during tension testing and fracture of a microspecimen. (a) The specimen was initially free of cracks. (b) As the tensile load was applied, a crack eventually formed at a specimen edge, near a fillet. (c) The crack propagated a short distance as the tensile load was increased. (d) The microspecimen fractured abruptly across the gage section.

underwent extensive plastic deformation prior to rupture, as seen in Figure 5b,c. This is consistent with observations made by Biener et al.²¹ Numerous ligaments in Figure 5c have necked down to diameters less than 10 nm. It is also noteworthy that the plastic deformation of ligaments appears confined to a region within ~ 100 nm of the crack surfaces (i.e., 1 to 2 ligament/pore “cells”). The underlying ligaments, toward the left side of Figure 5c, are not visibly deformed. This suggests that

ligament deformation during cracking of np-Au is a highly localized process and does not significantly affect the neighboring structure as cracks propagate through the material. This localization of deformation is likely due to an inability of np-Au to store dislocations or undergo strain hardening in the ligaments. Au ligament surfaces have no oxide that can trap dislocations, which can therefore glide to the surface and escape. Dislocations are able to interact with each other in the nodes,²² but these

Table I. Summary of Tensile and Compressive Microspecimen Test Data*

Sample ID	Testing Modality	Elastic Modulus (GPa)	Yield/Fracture Strength (MPa)	Ultimate Strength (MPa)	Poisson's Ratio	Comments
S1	Tension	3.2	11	—	0.15 ± 0.02	Broke at fillet between gage and ears.
S1 #2	Tension	—	12/14	—	—	Broke in center of gage. No DIC data.
S2	Compression	—	—	21	—	Grips came into contact. Test stopped.
S2 #2	Compression	—	—	24	—	Specimen cracked and finally failed.
S3	Compression	2.7	15	29	0.17 ± 0.02	Specimen buckled.
S4 Tens	Tension	3.1	9.1	—	—	Broke at fillet between gage and ears.
S4 Comp	Compression	—	16	47	—	Reached the maximum load on stage.

*Note: Most tensile specimens fractured abruptly, with no apparent plastic deformation. Compression specimens exhibited a yield strength similar to the tensile fracture strength, but were able to carry much higher ultimate stresses. Measured elastic modulus was lower than expected. Poisson's ratio was the same in tension and compression. The error bounds for values of Poisson's ratio represent the cumulative uncertainties associated with strain measurement.

are thicker than the ligaments, which only enhances the localization of deformation within the ligaments, which experience higher stresses.

COMPRESSIVE BEHAVIOR

Brittle porous materials can exhibit tension-compression asymmetry in plastic deformation, depending on the material system and cell-level architecture (e.g., orientation of structural elements relative to the applied stress, nodal degrees of freedom).¹⁴ In the current study, microspecimens were also tested in compression to assess the influence of testing

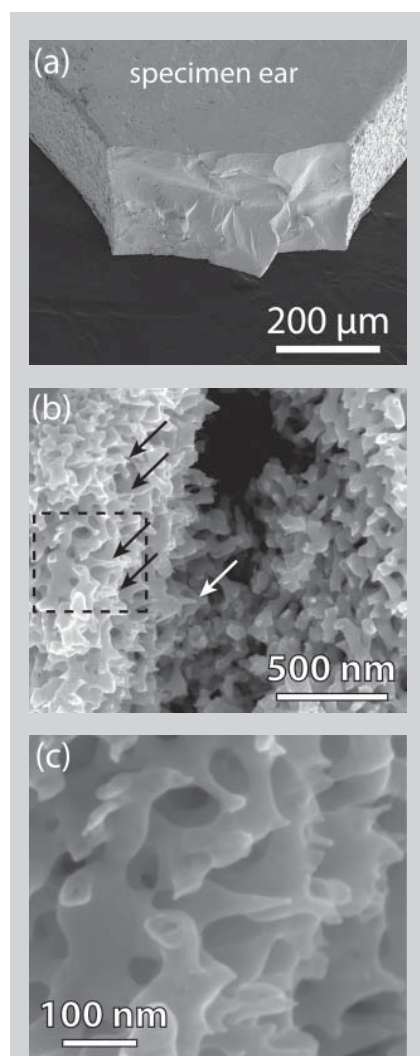


Figure 5. SEM micrographs of the fracture surface of a microspecimen subjected to tensile loading. (a) At the macroscale, fracture appears to have occurred in a brittle manner. At smaller length scales (b) and (c), the ductile failure of individual ligaments can be clearly seen. The high-magnification micrograph in (c), which corresponds to the dashed box region in image (b), shows several ligaments that underwent extensive necking prior to rupture.

modality on the mechanical response of np-Au. In the stress-strain curve of Figure 6, deviation from linear deformation occurred at 16 MPa, which was taken to be the compressive yield strength. This strength was also measured in another microspecimen, as shown in Table I. The maximum compressive stress reached in these tests was approximately 47 MPa, due to system limitations (the sample grips came into contact, or the maximum stage load was reached) or to buckling of the microspecimen. Thus, 47 MPa represents a lower bound for the ultimate compressive strength of bulk np-Au. Although the stress-strain behavior during compression becomes nonlinear and appears to indicate plastic deformation, we do not draw conclusions about intrinsic ductility from these tests, as other researchers have done.¹³ The closure of micro-cracks and the effects of misalignment-induced bending and buckling could contribute to the behavior measured here, and such mechanisms are not related to tensile ductility. The maximum strengths measured in compression were all higher than the tensile fracture strengths, which is not surprising given the brittle nature of np-Au. When loaded in tension, ligaments will neck and rupture, whereas they will bend and buckle when loaded in compression. The latter case allows for pore/ligament compaction and distribution of the applied load much better than the former case (tension), which concentrates it. Nonetheless, the compressive yield strength (15 MPa on average) is close to the tensile fracture strength (11 MPa on average), suggesting that plastic deformation of np-Au begins at much lower stresses than previously reported.¹⁰⁻¹² These lower strength levels do, however, agree with results from three-point bend tests⁷ and more traditional compression testing.¹³

Some literature studies have claimed that the hardness of np-Au is equal to the (ultimate) compressive strength,^{10,23} based on the behavior of cellular materials with low density and μm to mm-scale porosity.¹⁴ More recently, however, Jin et al. found a more traditional relationship between hardness and 1% offset yield strength ($H = 3\sigma_y$) based on indentation and compression testing of bulk np-Au.¹³ In the current study, some microspecimens were subjected to mi-

croindentation after they were dealloyed, prior to performing tension/compression testing, and yielded an average Vickers hardness $H = 145$ MPa. This is roughly three times the maximum compressive stress measured here, but that value of 47 MPa is a lower limit for the ultimate strength in compression. As discussed below, the elastic properties measured here would suggest a hardness-strength ratio close to the Tabor relation, which would agree with the hardness and maximum compressive stress values measured here. Comparison of the mechanical test data indicates that hardness is approximately one order of magnitude higher than the initial yield strength (i.e., 145 MPa versus 11 to 15 MPa for tension and compression, respectively). In light of these results and the recent study by Jin et al.,¹³ indentation hardness values may correlate with the ultimate compressive strength, but they do not represent a direct measure of np-Au yield strength.

ELASTIC PROPERTIES

Young's modulus was measured for three np-Au microspecimens, and the values were similar in tension and compression. As indicated in Table I, the tensile modulus was ~15% higher than the compressive modulus, although this difference may not be statistically significant. Further testing is required. However, the elastic modulus of cellular materials is generally higher in tension than in compression,¹⁴ due to beam-column interactions between ligaments oriented perpendicular and parallel to the loading axis.

Poisson's ratio, calculated from direct measures of the biaxial strain state, was similar in tension and compression. However, the average value of $\nu = 0.16$ lay between that of fully dense Au ($\nu = 0.44$)²⁴ and a low-density cellular solid ($\nu = 0$).¹⁴ This value is also much higher than that reported by Jin et al.,¹³ whose compression tests indicated a Poisson's ratio less than 0.08. Additionally, a non-zero Poisson's ratio implies that hardness cannot be equal to the yield strength, i.e. the plastic zone is somewhat constrained by the surrounding material into which it moves. In fact, as Poisson's ratio increases from zero, the ratio of hardness/strength increases rapidly from unity toward the standard

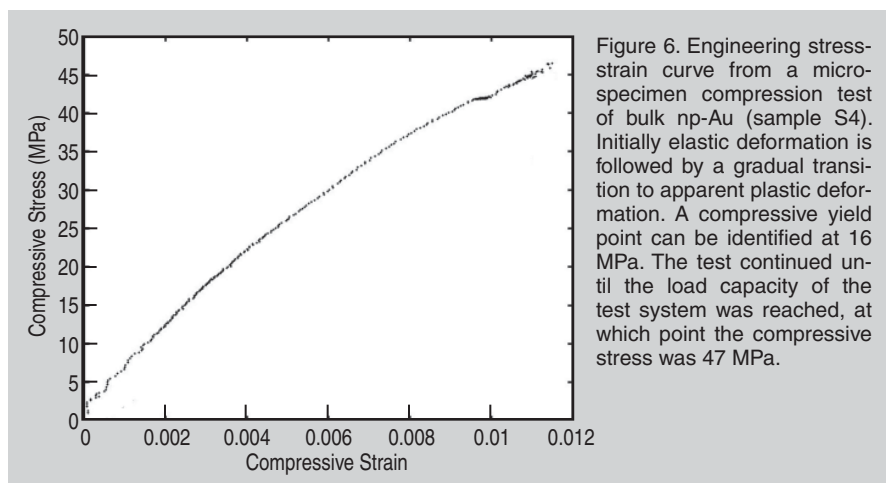
ACKNOWLEDGEMENTS

This material is based upon work supported by the National Science Foundation under Grant No. DMR-0847693 and Grant No. DMR-0413803. Acknowledgment is made to the Donors of the American Chemical Society Petroleum Research Fund (Grant No. 43324-G10), for support of this research. The financial support of the Deutsche Forschungsgemeinschaft GZ: SFB499/3-2007 is greatly acknowledged.

References

1. Y. Ding, M. Chen, and J. Erlebacher, *Journal of the American Chemical Society*, 126 (2004), p. 6876.
2. J. Erlebacher et al., *Nature*, 410 (2001), p. 450.
3. J.-F. Huang and I.W. Sun, *Advanced Functional Materials*, 15 (2005), p. 989.
4. S.O. Kucheyev et al., *Applied Physics Letters*, 89 (2006), p. 53102.
5. M.B. Cortie et al., *Sensors and Actuators B (Chemical)*, 123 (2007), p. 262.
6. F. Yu et al., *Analytical Chemistry*, 78 (2006), p. 7346.
7. R. Li and K. Sieradzki, *Physical Review Letters*, 68 (1992), p. 1168.
8. S. Parida et al., *Physical Review Letters*, 97 (2006), p. 035504.
9. Y. Sun and T.J. Balk, *Scripta Materialia*, 58 (2008), p. 727.
10. J. Biener et al., *J. Appl Phys*, 97 (2005), p. 024301.
11. J. Biener et al., *Nano Letters*, 6 (2006), p. 2379.
12. C.A. Volkert et al., *Applied Physics Letters*, 89 (2006), p. 61920.
13. H.J. Jin et al., *Acta Materialia*, 57 (2009), p. 2665.
14. L.J. Gibson and M.F. Ashby, *Cellular Solids - Structure and Properties* (New York, NY, Cambridge University Press, 1997).
15. K.J. Hemker and W.N. Sharpe, *Annual Review of Materials Research*, 37 (2007), p. 93.
16. D.S. Gianola et al., *Acta Materialia*, 54 (2006), p. 2253.
17. W.H. Peters and W.F. Ranson, *Optical Engineering*, 21 (1982), p. 427.
18. T.C. Chu et al., *Experimental Mechanics*, 25 (1985), p. 232.
19. H.A. Bruck et al., *Experimental Mechanics*, 29 (1989), p. 261.
20. C. Eberl, D.S. Gianola, and R. Thompson, *Digital Image Correlation and Tracking* (Mathworks file exchange server, File ID:12413, 2006).
21. J. Biener, A.M. Hodge, and A.V. Hamza, *Applied Physics Letters*, 87 (2005), p. 121908.
22. Y. Sun et al., *JOM*, 59 (9) (2007), p. 54.
23. A.M. Hodge et al., *Acta Materialia*, 55 (2007), p. 1343.
24. R.W. Hertzberg, *Deformation and Fracture Mechanics of Engineering Materials* (New York: John Wiley & Sons, Inc, 1989).

T. John Balk and Ye Sun are with the University of Kentucky, Chemical and Materials Engineering, Lexington, KY; Chris Eberl is with Karlsruhe Institute of Technology, izbs, Karlsruhe, Germany; Eberl and Kevin J. Hemker are also with The Johns Hopkins University, Mechanical Engineering, Baltimore, MD; and Daniel S. Gianola is with Forschungszentrum Karlsruhe, Institut für Materialforschung II, Karlsruhe, Germany, and the University of Pennsylvania, Materials Science and Engineering, Philadelphia, PA. Dr. Balk can be reached at (859) 257-4582; e-mail balk@engr.uky.edu.



quoted value of 3. For $\nu = 0.16$, the ratio is ~ 2.5 .¹⁴ It should be emphasized, however, that the elastic property measurements reported here need to be augmented by additional testing in order to obtain statistically reliable values.

SCALING BEHAVIOR

Based on the experimental results presented here, the strength and modulus of bulk np-Au appear to be significantly lower than previously reported for nanoindentation^{10,23} and micropillar compression tests.¹² If Gibson-Ashby scaling equations¹⁴ were to be applied, the equivalent bulk mechanical properties would be correspondingly lower. For materials with macroscale porosity, the yield strength of an open-cell foam is given by $\sigma_y = C_1 \sigma_s (\rho_{np}/\rho_s)^n$, where σ_s and ρ_s are the yield strength and density of solid Au, and ρ_{np} is the density of np-Au. C_1 and n are empirical constants, with $C_1 = 0.3$ and $n = 3/2$. Such scaling relations, developed for materials with porosity at larger length scales than that of np-Au, are the only ones currently available. Thus the yield strengths of bulk np-Au measured here ($\sigma_y = 11$ MPa in tension and 15 MPa in compression) would correspond to equivalent bulk strengths ranging from 220 MPa (tension) to 300 MPa (compression). These calculated values are significantly lower than those reported in the literature, which approach¹² the theoretical strength of Au.

Applying the scaling relation for elastic modulus should be straightforward. For open-cell materials with macroscale porosity, $E = E_s (\rho_{np}/\rho_s)^m$, where E_s is the modulus of solid Au and m is an empirical constant; typically, $m = 2$. The elastic modulus of dense Au is 78 GPa,²⁴

resulting in an expected modulus of 7.0 GPa for np-Au with a relative density of 30%. The actual measured values of np-Au modulus are ~ 3 GPa, implying that the standard scaling equation does not apply to the np-Au tested here.

These results are expected to have implications regarding the structural modeling of these porous architectures, which would affect our ability to estimate stresses at the ligament level. The standard Gibson-Ashby scaling equations were developed for materials with μm to mm -scale porosity and low relative density (up to 30% density, although most materials taken as supporting examples have lower density than this).¹⁴ Above 30% density, ligaments become so short and squat that the structural models, upon which these scaling relations are based, no longer apply. Nonetheless, these scaling relations are usually invoked for np-Au, although it is not yet clear how applicable they are to materials with nanoscale ligaments that are likely influenced by mechanical size effects. One study by Hodge et al.²³ proposed a modified scaling equation, by introducing a Hall-Petch term to the yield strength. The differences in measured and equivalent (scaled) mechanical properties reported here and in the literature may be due to differences in nanoscale structure. For future work, the impact of ligament morphology (short and squat, instead of long and slender) as well as size effects on plastic deformation mechanisms need to be considered. Overall, the discrepancies discussed here reveal a need for more detailed studies of the mechanical behavior of nanoporous materials, with a critical assessment of the applicability of porous material scaling equations.